

## Electronic Supplementary Information

### Probing the bifunctional catalytic activity of ceria nanorods towards the cyanosilylation reaction

Gonghua Wang,<sup>a,†</sup> Lu Wang,<sup>b</sup> Xiang Fei,<sup>a,\*</sup> Yunyun Zhou,<sup>a</sup> Renat F. Sabirianov,<sup>b</sup> Wai Ning Mei<sup>b</sup>  
and Chin Li Cheung<sup>a,\*</sup>

<sup>a</sup>*Department of Chemistry and Nebraska Centre for Materials and Nanoscience, University of Nebraska-Lincoln, Lincoln, NE 68588, United States.*

<sup>b</sup>*Department of Physics, University of Nebraska at Omaha, Omaha, NE 68182, United States*

<sup>†</sup> *Current address: Department of Mechanical and Materials Engineering, University of Nebraska-Lincoln, Lincoln, NE 68588, United States.*

<sup>\*</sup>*Phone: 1-402-472-5172; Fax: 1-402-472-9402; Email: ccheung2@unl.edu; xfei@huskers.unl.edu*

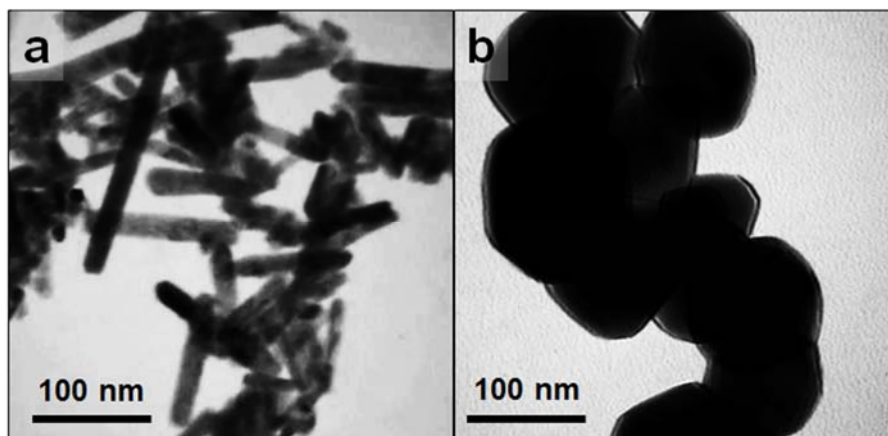


**Fig. S1** TEM images of ceria catalysts before activation: (a) as-synthesized ceria nanorods and (b) as-purchased bulk ceria.

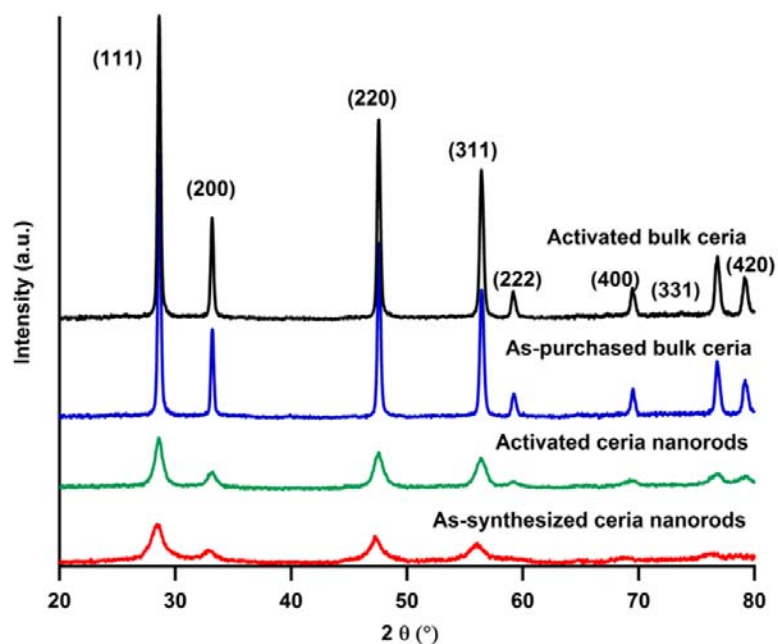


**Fig. S2** XRD patterns of ceria catalysts: (red) as-synthesized ceria nanorods, (green) activated ceria nanorods, (blue) as-purchased bulk ceria and (black) activated bulk ceria. XRD peaks are indexed according to ICDD card 04-013-4361 with respect to the cubic  $Fm\bar{3}m$  structure of cerium (IV) oxide ( $\text{CeO}_2$ ).

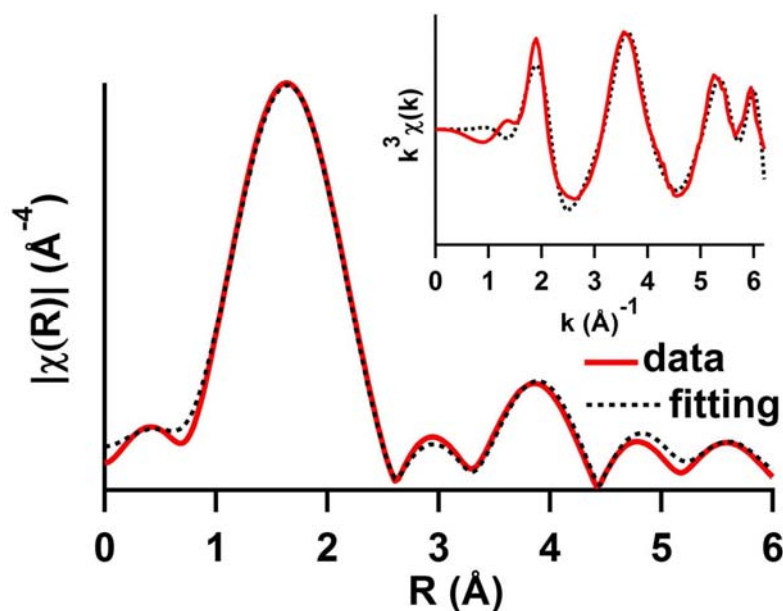


**Fig. S3** Fourier transformed Ce  $L_3$ -edge EXAFS data of unactivated ceria nanorods. The inset data are the corresponding EXAFS functions in  $k$  space. (Red lines: data; black dotted lines: fittings.)

**Table S1** Parameters of the local structure around Ce atoms obtained from curve fitting of the Ce  $L_{III}$ -edge EXAFS for unactivated and activated ceria nanorods and bulk ceria.

Sample	Bond	N	R (Å)	$\sigma$ ( $10^{-3} \text{Å}^2$ )	$\Delta E$ (eV)
Unactivated ceria nanorods	Ce-O	$7.0 \pm 0.1$	$2.11 \pm 0.01$	$8.7 \pm 1.5$	$-0.84 \pm 0.57$
	Ce-Ce	$7.7 \pm 0.2$	$3.92 \pm 0.02$	$17.4 \pm 5.2$	$-2.68 \pm 1.51$
	Ce-O	$18.4 \pm 2.1$	$4.44 \pm 0.02$	$15.1 \pm 4.9$	$-1.68 \pm 0.14$
Activated ceria nanorods <sup>a</sup>	Ce-O	$6.3 \pm 0.1$	$2.29 \pm 0.01$	$2.4 \pm 0.2$	$2.5 \pm 0.2$
	Ce-Ce	$7.4 \pm 0.4$	$3.82 \pm 0.01$	$2.2 \pm 0.5$	$-0.2 \pm 0.4$
	Ce-O	$14.7 \pm 1.2$	$4.52 \pm 0.01$	$3.4 \pm 0.5$	$0.8 \pm 0.4$
Bulk ceria <sup>a</sup>	Ce-O	$8.0 \pm 0.1$	$2.32 \pm 0.01$	$0.1 \pm 0.2$	$5.8 \pm 0.2$
	Ce-Ce	$12.0 \pm 0.3$	$3.82 \pm 0.01$	$0.1 \pm 0.5$	$-0.8 \pm 0.4$
	Ce-O	$24.0 \pm 1.2$	$4.48 \pm 0.01$	$1.5 \pm 0.5$	$1.6 \pm 0.4$

**Notes:** <sup>a</sup> Data for similarly prepared samples reported in reference 2b of the text.

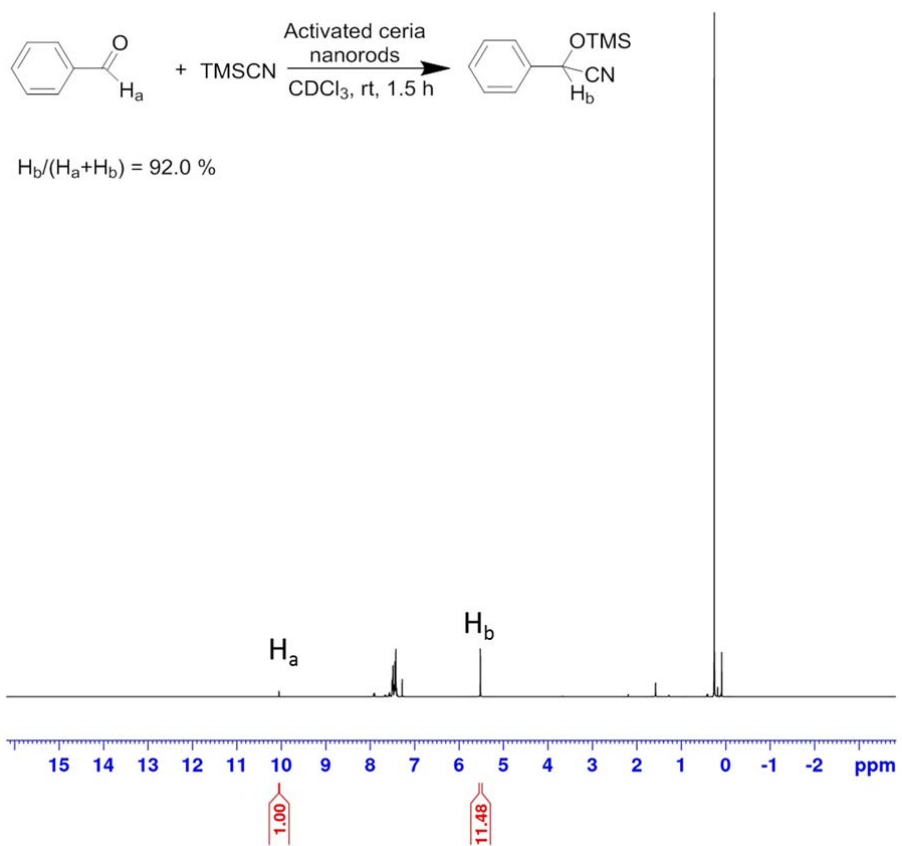


**Fig. S4** NMR spectrum of the reaction mixture for reaction between benzaldehyde and TMS-CN in Table 2 Entry 1 catalyzed by activated ceria nanorods after 1.5 hours of reaction time.

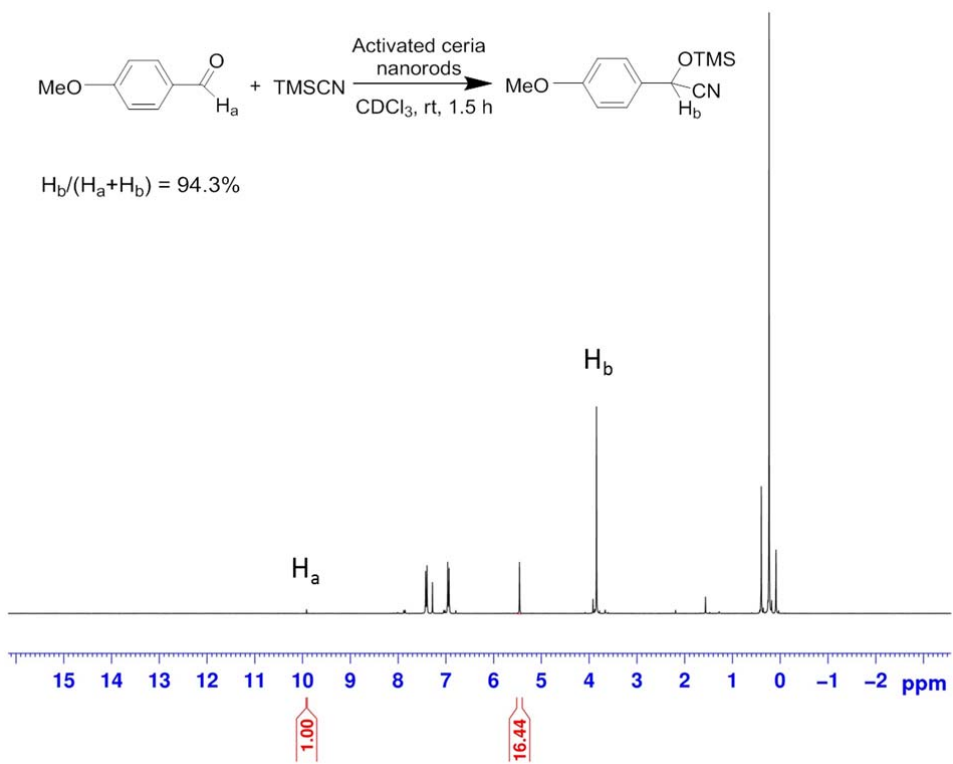


**Fig. S5** NMR spectrum of the reaction mixture for reaction between 4-methoxybenzaldehyde and TMSCN in Table 2 Entry 2 catalyzed by activated ceria nanorods after 1.5 hours of reaction time.

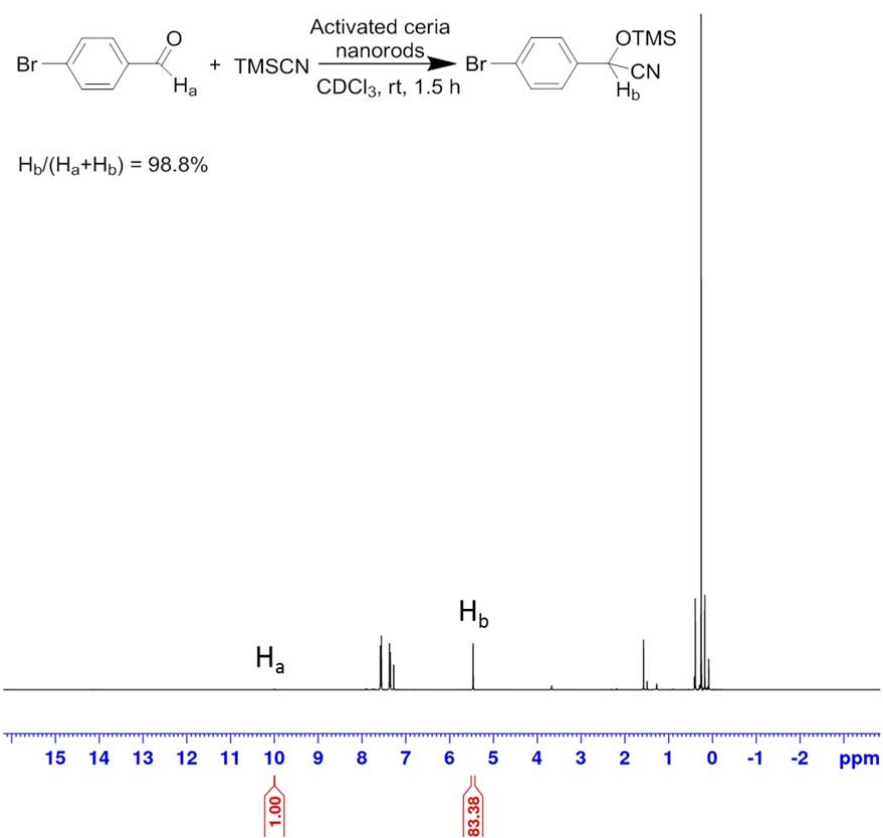


**Fig. S6** NMR spectrum of the reaction mixture for reaction between 4-bromobenzaldehyde and TMS-CN in Table 2 Entry 3 catalyzed by activated ceria nanorods after 1.5 hours of reaction time.

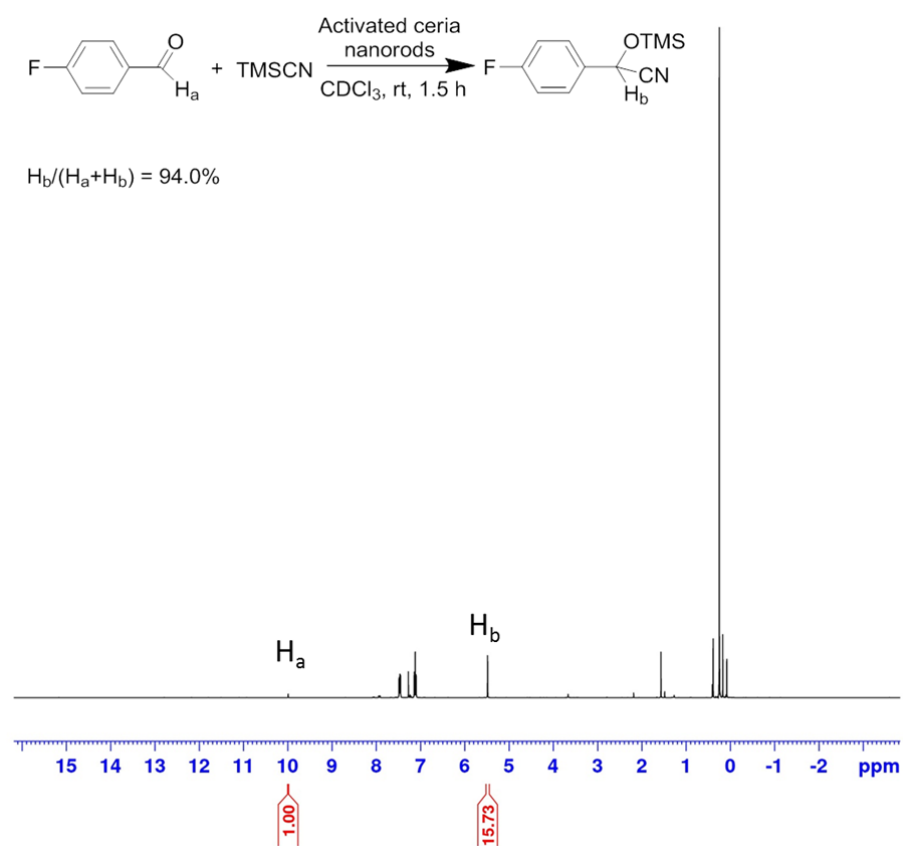


**Fig. S7** NMR spectrum of the reaction mixture for reaction between 4-fluorobenzaldehyde and TMSCN in Table 2 Entry 4 catalyzed by activated ceria nanorods after 1.5 hours of reaction time.

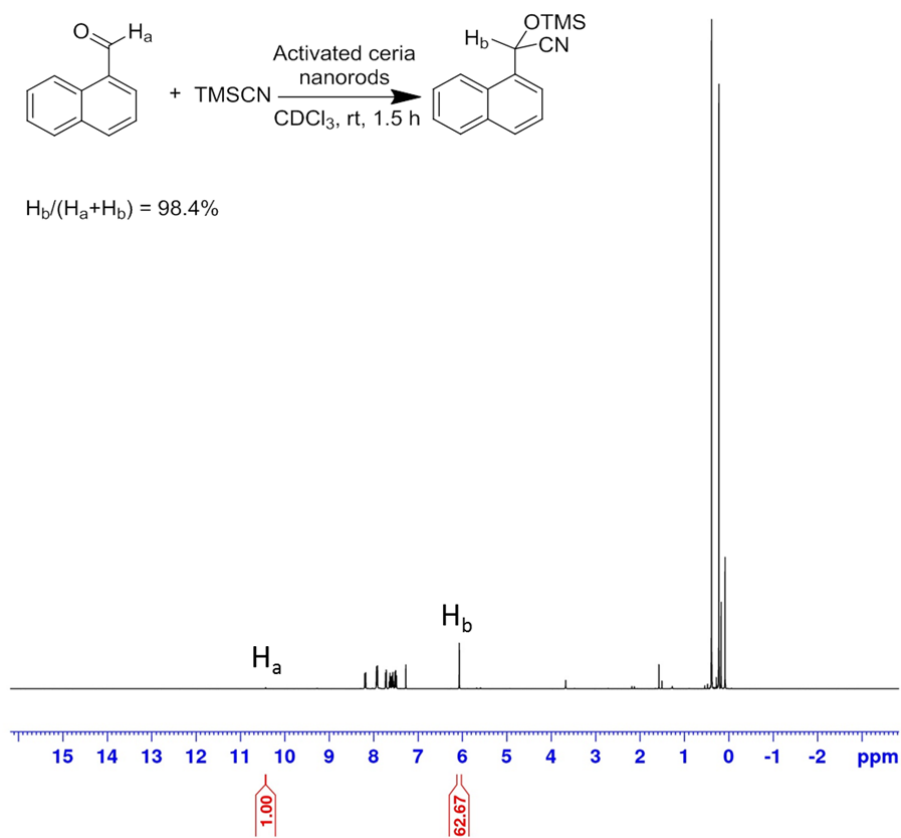
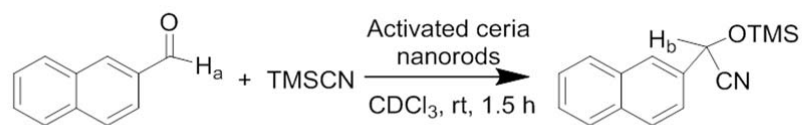


**Fig. S8** NMR spectrum of the reaction mixture for reaction between 1-naphthaldehyde and TMSCN in Table 2 Entry 5 catalyzed by activated ceria nanorods after 1.5 hours of reaction time.



Yield > 99%

The chemical shift for  $H_a$  is not detected.

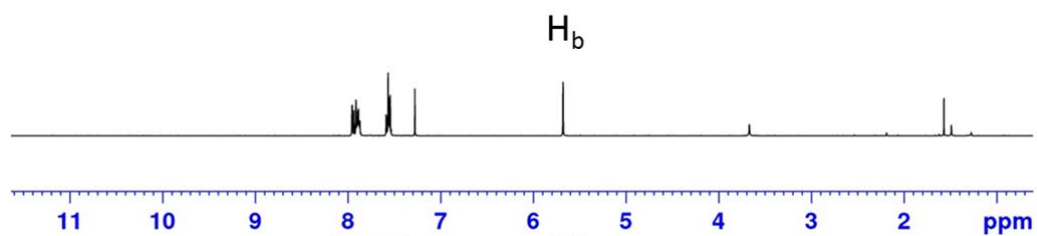
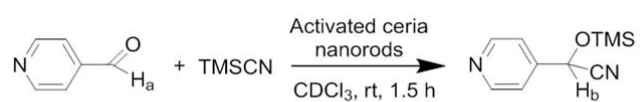


**Fig. S9** NMR spectrum of the reaction mixture for reaction between 2-naphthaldehyde and TMSCN in Table 2 Entry 6 catalyzed by activated ceria nanorods after 1.5 hours of reaction time.



Yield > 99%

The chemical shift for  $H_a$  is not detected.

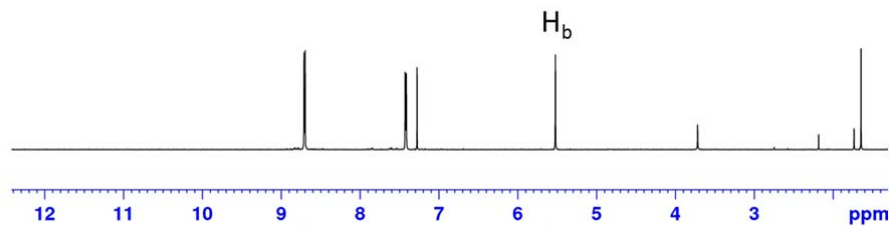


**Fig. S10** NMR spectrum of the reaction mixture for reaction between isonicotinaldehyde and TMSCN in Table 2 Entry 7 catalyzed by activated ceria nanorods after 1.5 hours of reaction time.

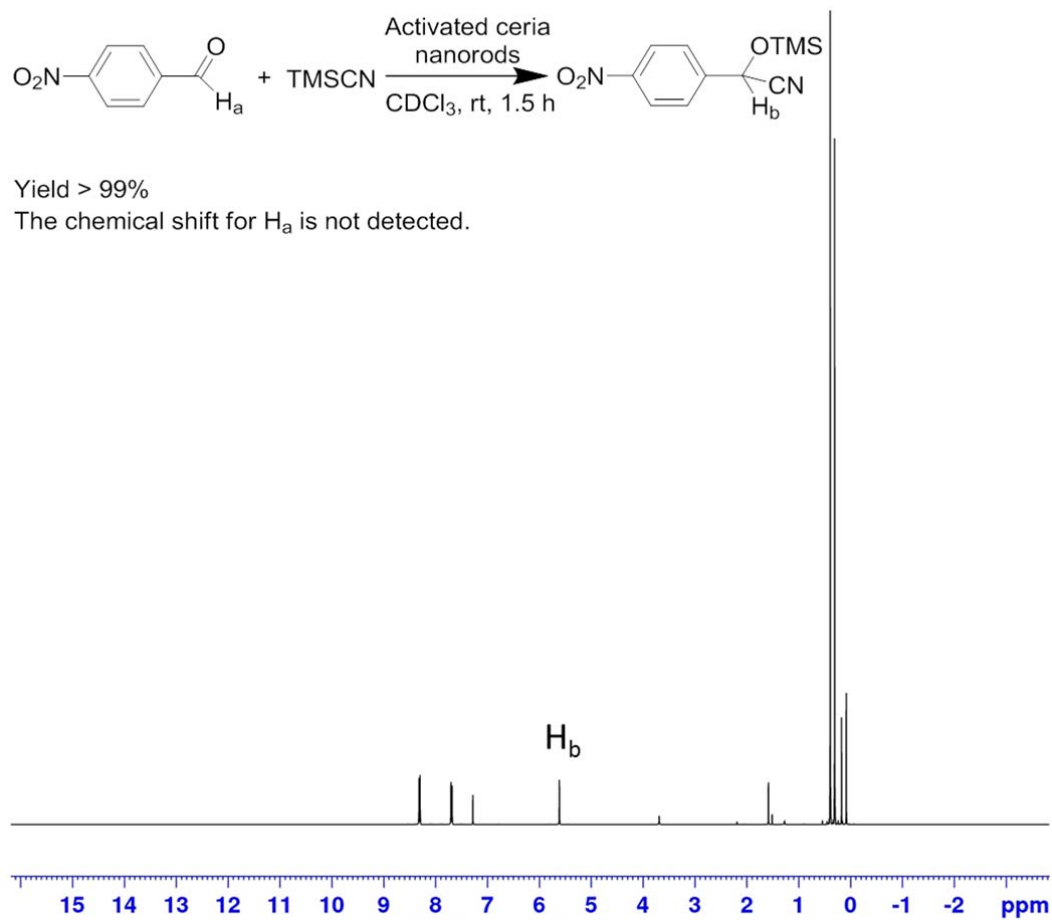


**Fig. S11** NMR spectrum of the reaction mixture for reaction between 4-nitrobenzaldehyde and TMS-CN in Table 2 Entry 8 catalyzed by activated ceria nanorods after 1.5 hours of reaction time.

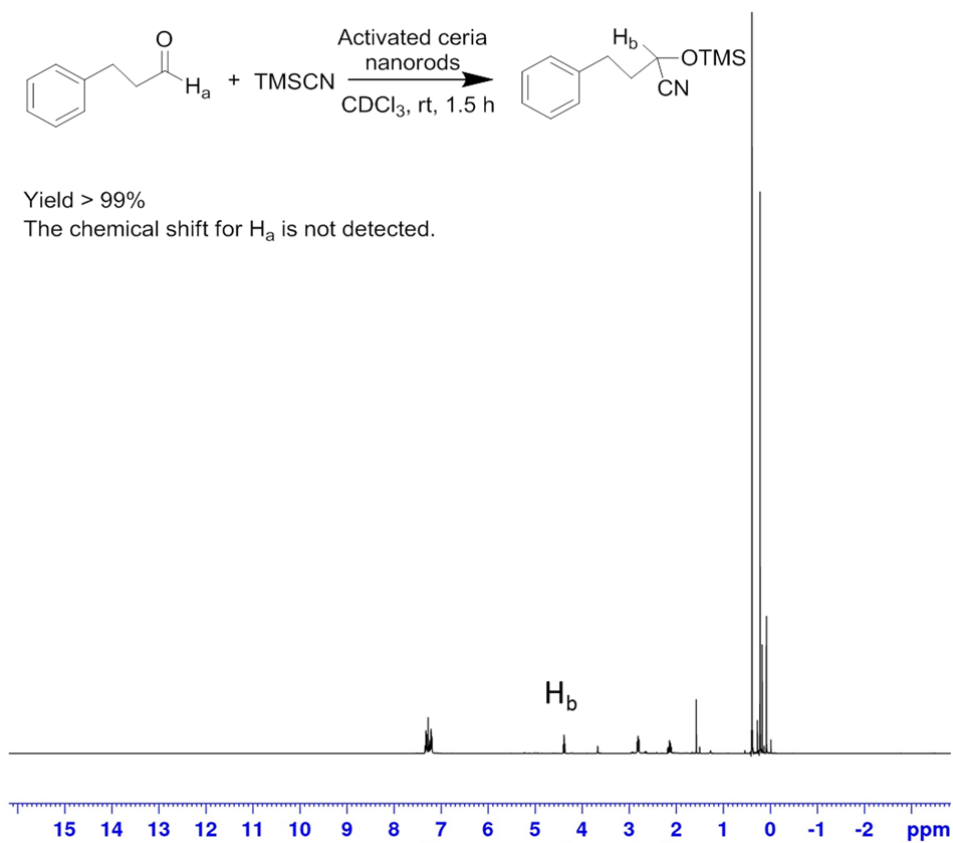


**Fig. S12** NMR spectrum of the reaction mixture for reaction between 3-phenylpropanal and TMSCN in Table 2 Entry 9 catalyzed by activated ceria nanorods after 1.5 hours of reaction time.

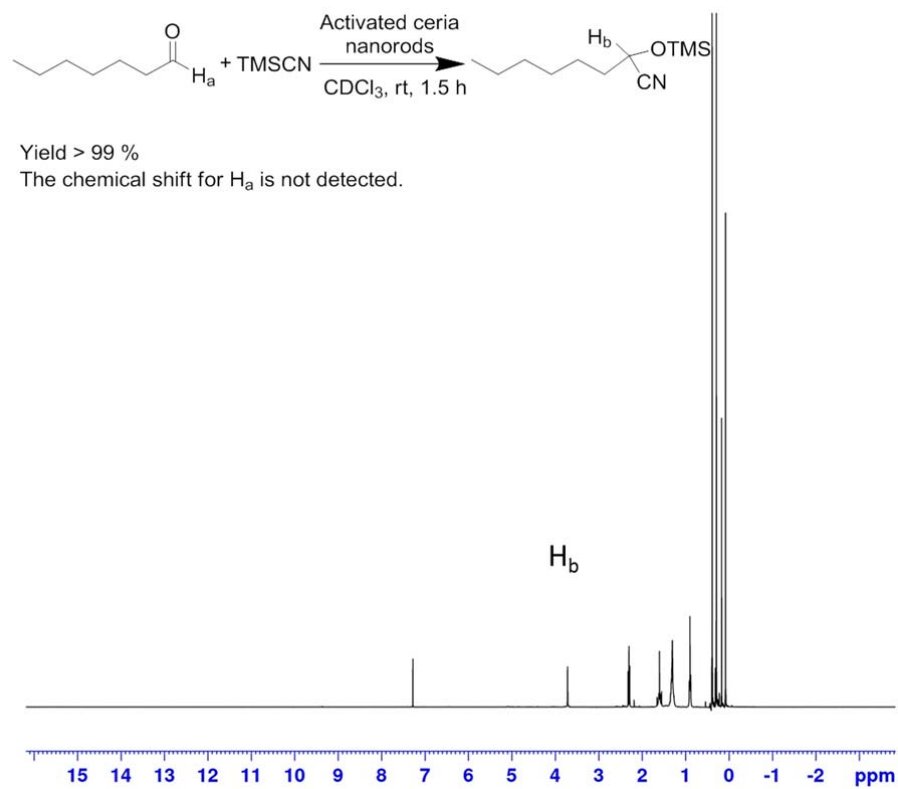


**Fig. S13** NMR spectrum of the reaction mixture for reaction between heptanal and TMSCN in Table 2 Entry 10 catalyzed by activated ceria nanorods after 1.5 hours of reaction time.

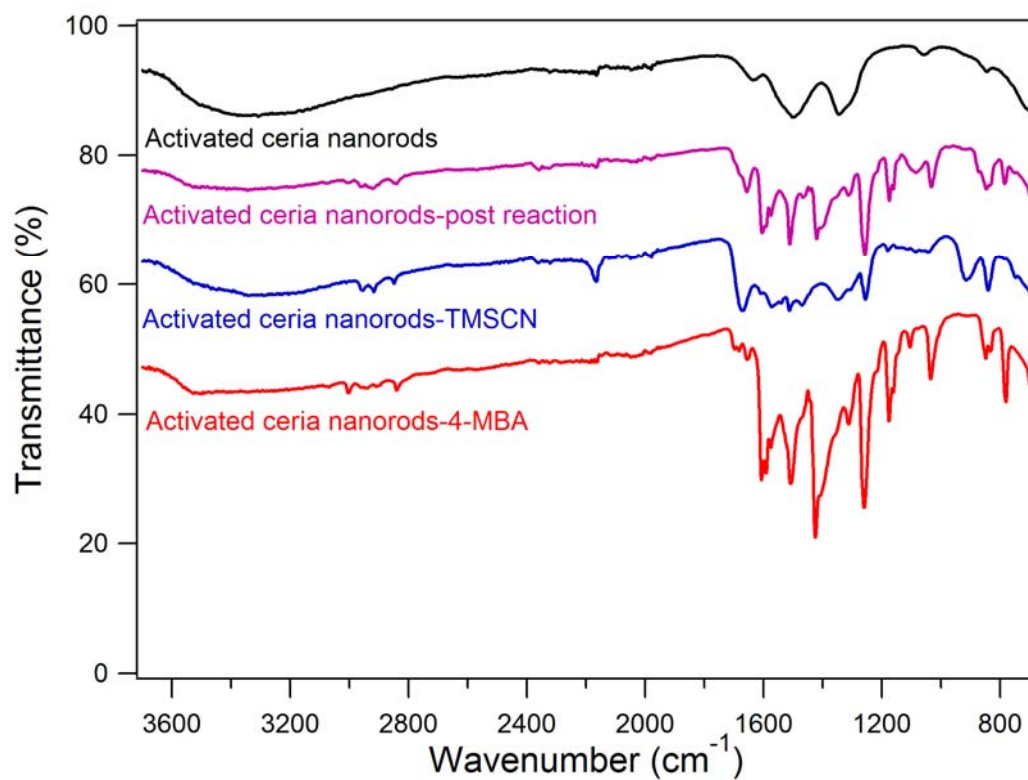


**Fig. S14** FTIR spectra of activated ceria nanorods catalyst, the post-reaction catalyst, and the catalysts after impregnation in 4-MBA and TMSCN. The spectra are shifted downward for presentation clarity.

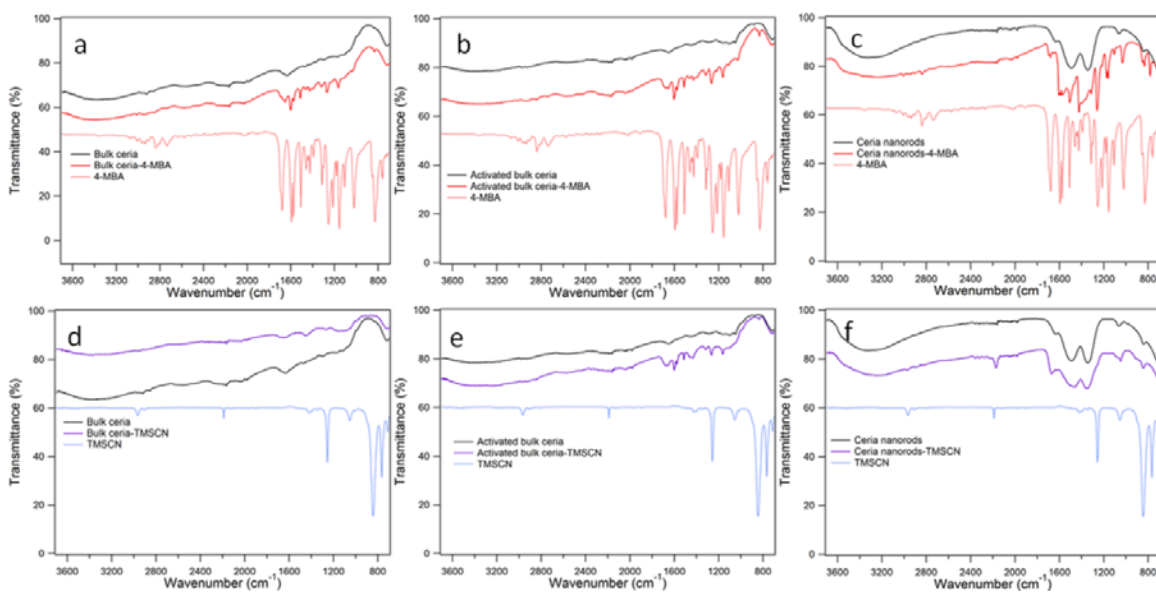


**Fig. S15** FTIR spectra of bulk ceria, activated bulk ceria, unactivated ceria nanorods before and after impregnation in (a-c) 4-MBA or (d-f) TMSCN. The spectra of 4-MBA and TMSCN are displayed for comparisons. The spectra are shifted downward for presentation clarity.

**Table S2** The infrared absorption frequency correlation table for the infrared spectra in Fig. 3, S14 and S15.

Wavenumber (cm <sup>-1</sup> )	Vibration <sup>1,2</sup>
3000-2800	CH <sub>3</sub> C-H stretch
2740	C-H stretch in aldehyde
2190, 2166	C≡N stretch
1680	C=O stretch in aldehyde
1606, 1591, 1508	C-C stretches in the benzene ring
1419	CH <sub>3</sub> twist
1356	CH <sub>3</sub> wag
1257	Si-CH <sub>3</sub> umbrella
1055	Si-O-Si asymmetric stretch
912	Silanol Si-O stretch
841	Si-CH <sub>3</sub> rock

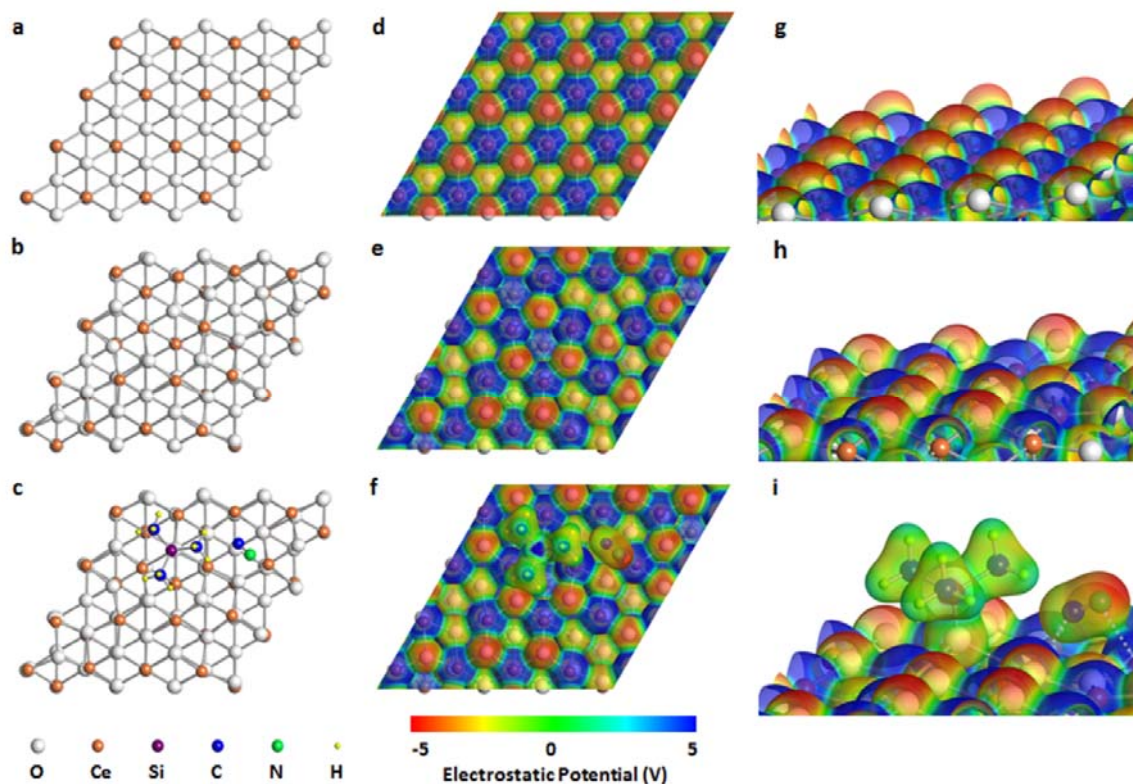


**Fig. S16** Structures of (a) CeO<sub>2</sub> slab, (b) CeO<sub>2-x</sub> slab and (c) TMSCN adsorbed on the CeO<sub>2-x</sub> slab. Isosurfaces of electron density (isovalue = 0.2 electron/Å<sup>3</sup>) of the three models color-coded with the electrostatic potential are illustrated from (d, e, f) top view and (g, h, i) zoomed-in angled view, respectively. The negative electrostatic potential around O-sites illustrates that O atoms are negatively charged, particularly that the surface O atoms are even more negatively charged than the subsurface ones. The positive electrostatic potential around Ce-sites suggests that the Ce atoms are positively charged.

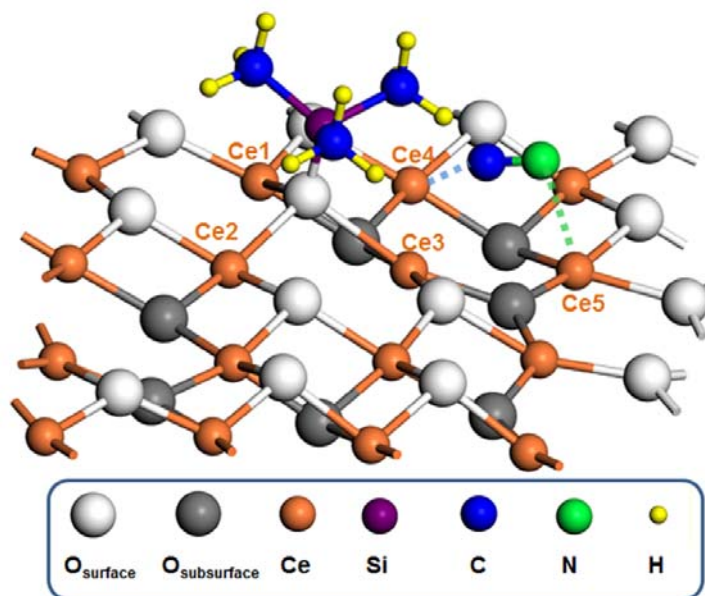


**Fig. S17** Side view of the optimized structure of a TMSCN molecule chemisorbed on the CeO<sub>2-x</sub> slab in the ball-and-stick representation.

**Table S3** Interatomic bond lengths (Å) in CeO<sub>2-x</sub> slab, TMSiCN and TMSiCN adsorbed on the CeO<sub>2-x</sub> slab model.

Interatomic bond lengths (Å)	Ce(1)-O	Ce(2)-O	Ce(3)-O	O-Si	Si-C (N)	C-N	Ce(4)-C	Ce(5)-N
CeO <sub>2-x</sub>	2.48	2.37	2.49	-	-	-	-	-
TMSiCN	-	-	-	-	1.86	1.17	-	-
TMSiCN adsorbed on CeO <sub>2-x</sub>	2.61	2.62	2.74	1.68	4.57	1.19	2.82	2.66

**Table S4** Binding energies and atomic charges of individual atoms in the adsorption models.

Models	Binding Energy (eV)	Charge (e)								
		Ce(1)	Ce(2)	Ce(3)	O	Si	C(N)	N	Ce(4)	Ce(5)
CeO <sub>2-x</sub>		2.69	2.68	2.74	-1.65	-	-	-	2.86	2.76
TMSiCN	-6.28	-	-	-	-	1.51	-0.28	-0.27	-	-
TMSiCN adsorbed on CeO <sub>2-x</sub>	-1.08	2.62	2.66	2.70	-1.42	1.54	-0.36	-0.51	2.85	2.78
CN detached from TMSiCN- CeO <sub>2-x</sub>	4.15	-	-	-	-	-	-0.44	-0.23	-	-
CN adsorbed on CeO <sub>2-x</sub>	-5.25	2.69	2.71	2.80	-1.64	-	-0.36	-0.54	2.86	2.78
TMS adsorbed on CeO <sub>2-x</sub>	-2.11	2.61	2.64	2.72	-1.42	1.53	-	-	2.83	2.69

## References

- (1) Smith, B. C. *Infrared spectral interpretation: a systematic approach*; 1<sup>st</sup> ed.; CRC Press LLC: Boca Raton, Florida, 1998.
- (2) Thirupathi, B.; Patil, M. K.; Reddy, B. M. *Appl. Catal. A* 2010, **384**, 147-153.